A SIMPLIFIED RATIONAL APPROACH FOR THE PRELIMINARY ASSESSMENT OF THE EXCAVATION BEHAVIOUR IN ROCK TUNNELLING

G. Russo
Geodata SpA, Turin, Italy

ABSTRACT: This paper deals with the forecasting of the excavation behaviour of rock masses in tunnelling. In particular, a new multiple graph for a preliminary estimate is shown, in which different criteria and classification systems have been integrated. In a simplified but rational way the potential typical deformation phenomena (hazards) for tunnelling in rock are identified through the quantification, in a logical sequence, of fabric (1), strength (2), competency (3) and self-supporting capacity (4) of a rock mass. Based on this preliminary analysis, the tunnel design can consequently focus on the detected potential problems, implementing with the required detail the most adequate methods of analysis and calculations.

1 INTRODUCTION

The prediction of the excavation behaviour is a key point in tunnel design and many efforts have been done to increase the reliability of such an evaluation, as well as to classify the possible response of excavation in a rational and useful way.

As reported by Hencher (1994), according to Knill (1976) the engineering of ground behaviour should conceptually be assessed by the sequential equations reported in Tab.1.1.

Eq.1’	Material properties + Mass fabric = Mass properties
Eq.2’	Mass properties + Environment = Engineering geological situation
Eq.3’	Engineering geological situation + Influence of engineering works = Engineering of ground behaviour

Table 1.1: Engineering geology expressed by verbal equations (Knill, 1976).

In the present paper attention is more paid on the individuation of the potential hazards for tunnel excavation; therefore, on the one hand, some items are more detailed with respect to the example in Tab.1.1, but on the other hand the influence of the engineering works is not taken into consideration. In particular, a 4-sector graph (Fig.2.1) is presented for a sequential and schematic solution of the equations reported in Tab.1.2.

Eq.1	Rock block volume + Joint Conditions = Rock mass fabric
Eq.2	Rock mass fabric + Strength of intact rock = Rock mass strength
Eq.3	Rock mass strength + In situ stress = Competency
Eq.4	Competency + Self supporting capacity = Excavation behaviour (→Potential hazards)

Table 1.2: Logical frame adopted for the identification of the excavation hazards.

In the next section, such multiple graph, useful for the preliminary assessment of the excavation behaviour in rock, is described in detail, pointing out the relative background of each sector.

2 MULTIPLE GRAPH FOR THE PRELIMINARY ESTIMATE OF THE EXCAVATION BEHAVIOUR

As previously mentioned, the multiple graph is composed by 4 sectors, each of them finalized to a user-friendly quantification of the corresponding properties presented in Tab.1.2.
The complete reading of the graph proceeds clockwise from the bottom-right quadrant (I to IV). However, depending on the available information, the user may eventually start entering in one of the sectors: for example, if the GSI (Geological Strength Index, Hoek et al., 1995) is already assessed and detailed geo-structural data are not available, the start-off quadrant is II.

2.1 *Graph I: Estimation of Rock Mass Fabric*

Basic equation (Eq.1 of Tab.1.2; in parenthesis the considered parameters): Rock Block Volume (Vb) + Joint Conditions (jC) = Rock Mass Fabric (GSI).

When the rock mass can be reasonably treated as an equivalent-continuum, with isotropic geomechanical properties, the geo-structural features of rock masses can be expressed by a “fabric index” (Tzamos and Sofianos, 2006), which may be defined as a scalar function of two components: rock structure and joint condition. In the present case, the reference fabric index is the GSI and its estimate is derived by the method recently proposed by the author (“GRs” approach, Russo, 2007).

Such a new method for calculating the GSI has been developed taking into consideration the conceptual equivalence between GSI and JP (Jointing Parameter) of the RMi system (Palmstrom, 1996), considering that both are used to scale down the intact rock strength (σ_c) to rock mass strength (σ_{cm}).

In fact, according with the two systems, we have:

RMi: $\sigma_{cm} = \sigma_c{*}JP$ 1)

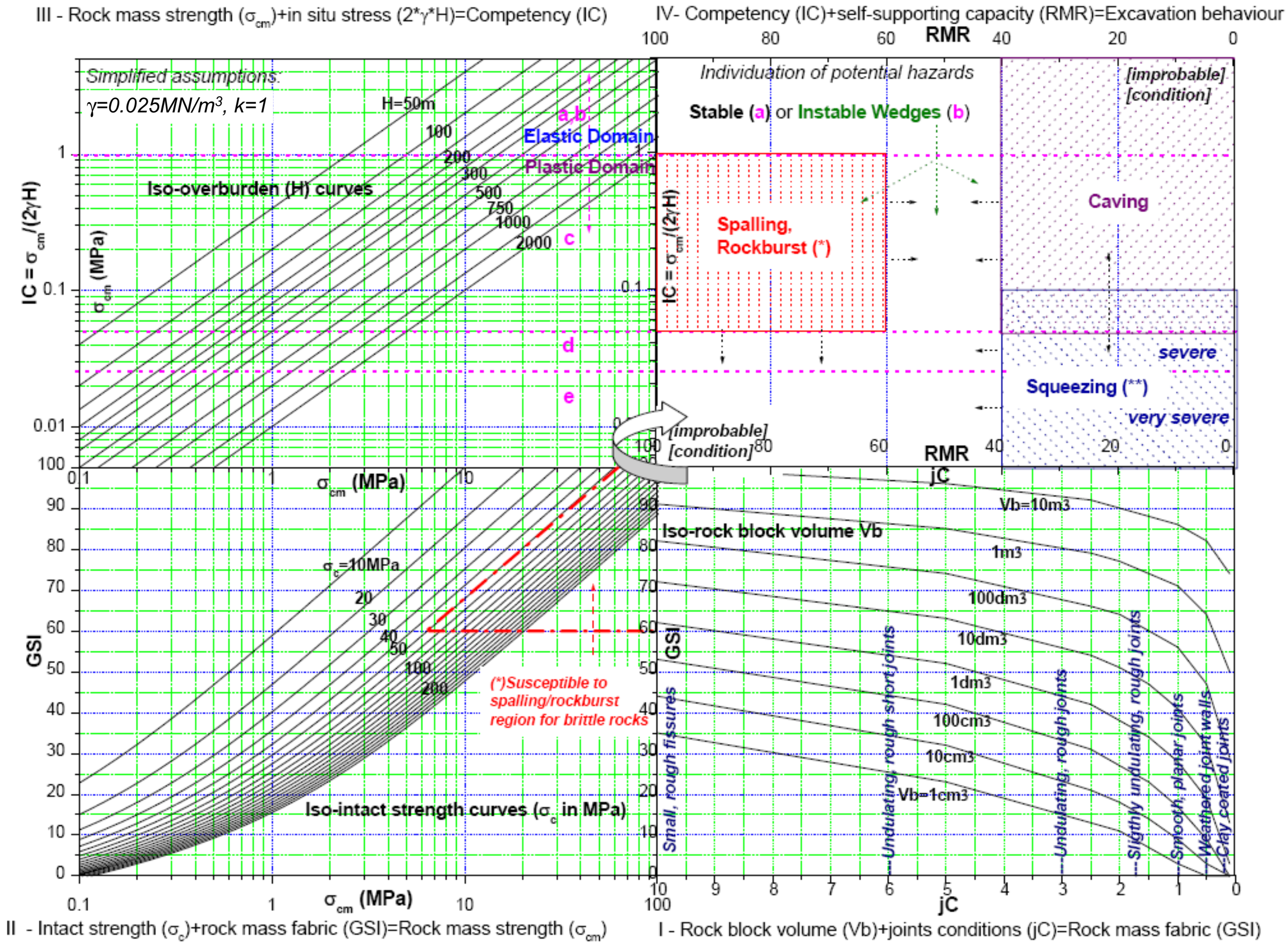

Fig. 2.1: Proposed multiple-graph for the preliminary setting of excavation behaviour. Notes: (*) Only for the susceptible to rockburst region for brittle rocks [IF=(σ_c/σ_t)>8], otherwise a shear type failure should occur; (**) squeezing involves pronounced time-dependent deformations and is associated to rocks with low strength and high deformability: otherwise, prevalent plastic deformations (non time-dependent) occur, generally associated to caving; squeezing depends also from the length of the potential prone zone: given a possible "silo effect", for short zones included in good quality rocks, a caving behaviour is most likely to occur. Symbols: σ_c, σ_{cm}= intact, rock mass strength (=σ_c*s^a); jC= joint condition factor, Vb= block volume; γ= rock mass density.

GSI: $\sigma_{cm} = \sigma_c * s^a$ 2)

where s and a are the Hoek-Brown constants.

Therefore, JP should be numerically equivalent to s^a and given that for undisturbed rock masses (Hoek et al., 2002) one has:

s = exp[(GSI-100)/9] and 3)

a = (1/2)+(1/6)*[exp(-GSI/15)-exp(-20/3)] 4)

a direct correlation between JP and GSI can be obtained, i.e.:

$JP=[\exp((GSI-100)/9)]^{(1/2)+(1/6)*[\exp(-GSI/15)-\exp(-20/3)]}$ 5)

For the inverse derivation, the perfect correlation (R^2 = 0.99995) can be used with a sigmoidal (logistic) function of the type:

$GSI = (A1-A2)/[1+(JP/X_o)^p]+A2$ 6)

with A1=-12.198; A2=152.965; X_o=0.191; p=0.443. Then $GSI \approx 153-165/[1+(JP/0.19)^{0.44}]$. 7)

Based on such a correlation, a "robust" quantitative estimation of the GSI can be made, by defining the parameters concurrent to the evaluation of JP, i.e. the block volume (Vb) and the Joint Condition factor (jC). A graphic representation of the described correlation is presented in Fig. 2.2

The sector I of the graph shown in Fig. 2.1 is derived from the above equations. The quantification of the Joint Condition Factor (jC) is based on published tables (see for example Palmstrom's web site www.rockmass.net, where a complete treatment of the RMi method can be found). Following the suggestion of Palmstrom (2000), some typical jC values are reported in the graph as well for a quick preliminary evaluation.

Finally, it should be noted that the use of the GRs approach is not recommended in complex and heterogeneous rock masses, such as a flysch, where the specific charts proposed by Marinos and Hoek (2001) may be a more opportune reference for calculating the GSI.

2.2 *Graph II: Estimation of rock mass strength*

Basic equation (Eq.2): Rock Mass Fabric (GSI) + Intact rock strength (σ_c) = Rock mass strength (σ_{cm}).

The estimation of the rock mass strength is based on the equations of Hoek et al. (2002), already presented above. In particular, such a value is graphically obtained by the intersection of the estimated GSI and intact strength curves. The reliability of the rock mass strength estimation is primarily related to both the effective applicability of the

Hoek-Brown failure criterion (→ homogeneous and isotropic medium) and the occurrence of shear type failure.
Differently, a "spalling type" failure, which involves intact rock strength, may occur when overstressing a good quality, hard and brittle rock mass. In such a case, according to the so called "m=0 approach" (see, for example, Kaiser (1994) and Diederichs (2004, 2005)), the mobilized strength at failure may result either higher and lower than the σ_{cm} derived by the GSI-based Hoek et al. equations, basically depending on the value of both the GSI itself and the stress for the cracks initiation.

For a preliminary estimation of the possibility of stress-driven instabilities of brittle rocks [Brittle Index IF= $(\sigma_c/\sigma_t)>8$], in the graph II, the region susceptible to spalling/rockburst, if in the presence of adequate stress conditions, is highlighted.

Taking into consideration the cited references, the lower boundaries of such a region have been taken in favour of safety as coincident with values of GSI and σ_c (MPa) both correspondent to 60. However, Diederichs (2005), for the same type of brittle rocks, classified the susceptibility as "medium" only for σ_c>80MPa.,

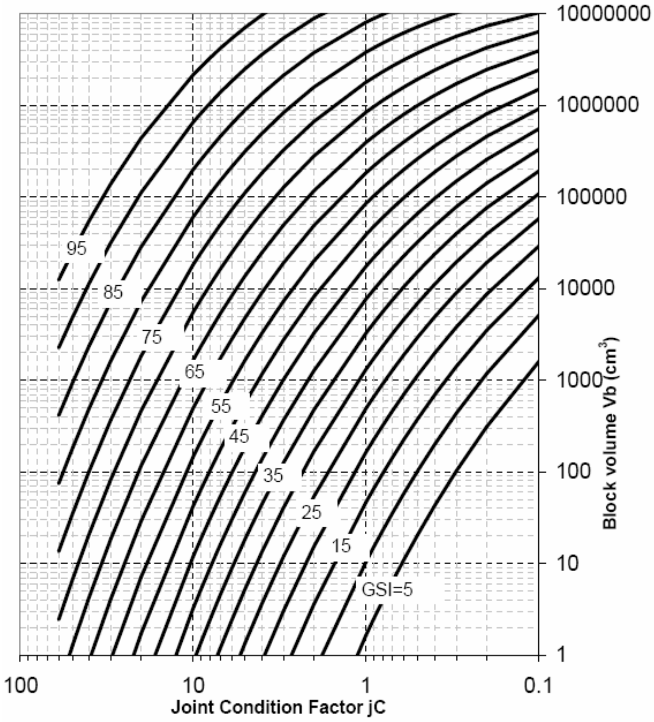

Fig. 2.2: Diagram for the assessment of GSI based on the RMi parameters jC and Vb ("GRs "approach, Russo, 2007). Note: It is suggested to set GSI=5 as the minimum value.

2.3 *Graph III: Estimation of rock mass competency*

Basic equation (Eq.3): Rock mass strength (σ_{cm}) + In situ stress (σ_θ) = Rock mass competency (IC).

The Competency Index (IC) is simply defined as the ratio between the rock mass strength (σ_{cm}) and the tangential stress (σ_θ) on the excavation contour.

It is important to note that a simplified assumption about the original in-situ stress is here adopted by considering a value of k=1, where k is the ratio between the in situ horizontal and vertical principal stresses.

Consequently, for a circular tunnel one has $\sigma_\theta = 2\gamma H$, with γ= rock mass density (assumed value = 0.025kN/m^3) and H= overburden. In the case of $k\neq1$ a reasonable approximation may consist in calculating the maximum tangential stress $\sigma_{\theta max}=3\sigma_1-\sigma_3$ and then divide the result by 2γ, in order to derive the fictitious overburden that origins the same $\sigma_\theta=\sigma_{\theta max}$ for k=1.

The value of IC=1 separates in the graph the deformation response of the excavation into the elastic (above) and plastic (below) domains.

Moreover, in the graph are also reported some horizontal dotted lines which represent the best correlation of the Competency Index with the behavioural classification reported in Fig.2.5.

As later presented, in such a classification ("GD") four classes (a/b, c, d, e/f) were originally identified (Russo et al., 1998) as function of both the radial deformation at the excavation face (δ_o) and the normalized extension of the plastic zone around the cavity (Rp/Ro).

Two further distinctions were considered: 1) in the case of elastic response (i.e. classes a/b) the class "b" indicated a discontinuous rock mass prone to wedge instability; 2) the class "f" was associated to conditions of immediate collapse of the tunnel face.

As treated in the next section, more recently the original GD-classification has been updated to better take into account the real discontinuous character of the rock masses and consequently to improve the prediction of different deformation phenomena, such as the gravitational type and the brittle, stress-driven instabilities (Figs. 2.4, 2.5; Russo and Grasso, 2006 and 2007).

To transfer such a classification on the graph, the characteristic line (C. Carranza T. solution, 2004) and the Monte Carlo methods have been implemented to find an approximate correlation between the IC and the GD-classes.

In particular, as reported in Fig. 2.3, a large variability of the input geomechanical parameters has been considered by referring to adequate uniform distribution. Moreover, for the calculations: *i*) a strain-softening behaviour has been considered by referring to the approach proposed by Cai et al. (2007) centred on the concept of "residual GSI" (GSI_{res}); *ii*) the rock mass modulus of deformability has been derived by the simplified equation proposed by Hoek and Diederichs (2006); *iii*) δ_o has been obtained by modifying the equation proposed by Hoek (1999, in Carranza, 2004) (see further explanation in the next section).

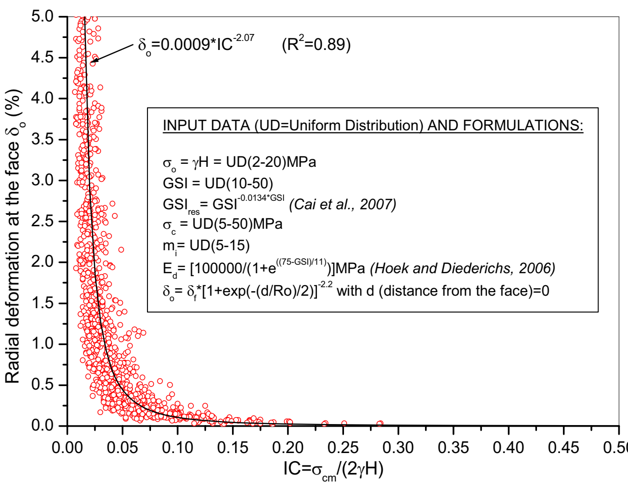

Fig.2.3: Correlation between the radial deformation at the face (δ_o) and the Competency Index (IC).

In Fig. 2.3, the results of 2000 iterations by the Latin Hypercube sampling method, as well as the best interpolating curve are shown for the relationship IC-δ_o. Moreover, the combined state of the two parameters involved in the GD-classification (i.e. δ_o and Rp/Ro) has been statistically analysed and the approximate correlation lines reported in the graph have been finally assessed.

Given the related uncertainty, they necessarily reflect only the most probable conditions for the parametrical variability assumed in the probabilistic calculation.

2.4 *Graph IV: Estimation of excavation behaviour*

Basic equation (Eq.4): Rock mass competency (IC) + Self supporting capacity (RMR) = Excavation Behaviour.

In the last quadrant of the multiple graph, the integrated behavioural classification is applied in approximate form, by using the previous correlations with IC.

Following the conceptual scheme presented in Fig. 2.4, the original GD-classification system has been integrated by the RMR classes (Bieniawski, 1984) considering also their well-known empirical relationship with the self-supporting capacity of the rock masses.

With the same logic of Fig. 2.5, some of the main hazards for tunnelling are consequently delimited in the new graph.

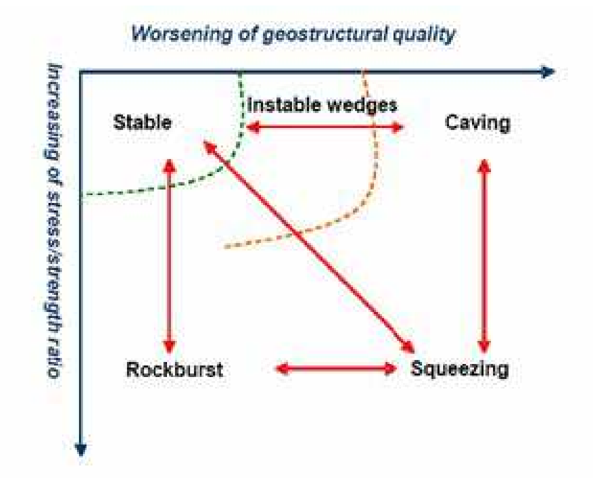

Fig.2.4: Conceptual scheme for a general setting of the ground behaviour upon excavation

The term *caving* is here used to identify generic gravitational collapse of portions of highly fractured rock mass from the cavity and/or tunnel face. Therefore, given their very poor self-supporting capacity, the highest risk of caving is associated to the most unfavourable RMR classes.

S*queezing (s.s.)* involves pronounced time-dependent deformations and is generally associated to rocks with low strength and high deformability such as, for example, phillytes, schists, serpentines, mudstones, tuffs, certain kinds of flysch, chemically alterated igneous rocks (Kovari, 1998). Otherwise, plastic deformations should prevail and caving is also probable. Further detailed analysis, based on a more accurate modelling of geomechanical properties, should be able to remark the just described distinction.

The terms "severe" and "very severe" have been associated to GD-classes "d" and "e", respectively. By considering also the type of stabilisation measures applied, they may be roughly related to the correspondent δ_f–based classes of squeezing proposed by Hoek and Marinos (2000), if one incorporates in the last term also the grade "extremely severe".

This position is supported by the observation that, for overstressed poor/weak rock-masses, δ_o is frequently found to be a minor percentage of the final radial deformation (δ_f) than commonly considered (i.e. $\delta_o \approx 0.3\delta_f$ as for Hoek, 1999), in particular when a *softening/creep* behaviour occurs.

For example, in several case-histories the equation in Fig. 2.3, derived by axi-symmentric numerical analysis, has fitted better the results of monitoring:

$$\delta_o = \delta_f \, [1+\exp(-(d/Ro)/2)]^{-2.2} \qquad 9)$$

where d=distance from the face.

In addition to the notes to Fig. 2.1, it is reasonable to expect an increase of the *rockburst* intensity with reduction of IC. For example, Palmstrom (1996), for massive brittle rock, with $\sigma_{cm} \approx \sigma_c/2$, gives indication of heavy rockburst when IC<0.5.

The potential of *rock wedge* failure is mainly associated to good (/fair) rock masses subjected to relatively low stress condition, i.e. when the response at excavation is dominated by the shear strength of discontinuities and a "translational" failure should occur (Bandis, 1997). Further detailed analyses, for example by using limit equilibrium methods, should verify the effective possibility of kinematical instabilities.

Two "improbable" zones have also been marked in the graph corresponding to unrealistic combinations between GSI and RMR: the first below the "spalling/rockburst" region and the other in the upper right part ("caving" zone), where RMR class V and elastic behaviour theoretically overlap.

3 PRACTICAL APPLICATION

In Fig. 3.1 the practical application of the multiple graph is illustrated, plotting in particular some significant case-histories, for which a comparison between the predicted and the observed behaviour can be assessed.

In Tab. 3.1. the essential data of such case-histories are schematically reported, including the type of the main counter-measures adopted for the stabilisation of the tunnel.

As shown in Fig.3.1, when applying the scheme of Fig.2.1 in practice, it is generally recommended not to focus on a single point of input, but to specify a possible range of variation of the input parameters to reflect the uncertainties involved.

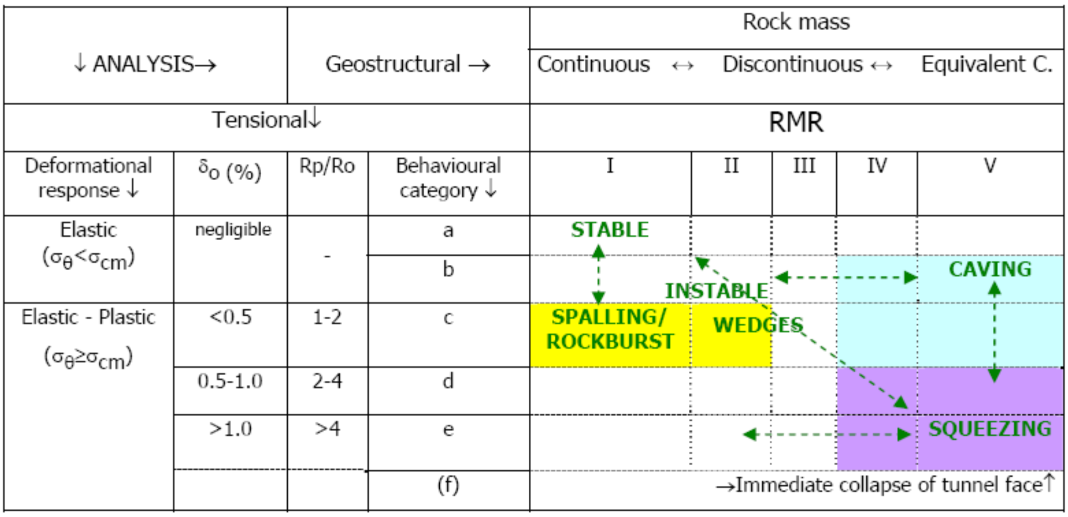

Fig.2.5: Classification scheme of the excavation behaviour (GD-classification, Russo and Grasso, 2006, 2007, modified).

Notes: δo=radial deformation at the face; Rp/Ro=plastic radius/radius of cavity; σ_θ=max tangential stress; σ_{cm}=rock mass strength. The limits of shadow zones are approximated and represent the most typical condition; see also the notes to Fig.2.1 and further explanations in the text.

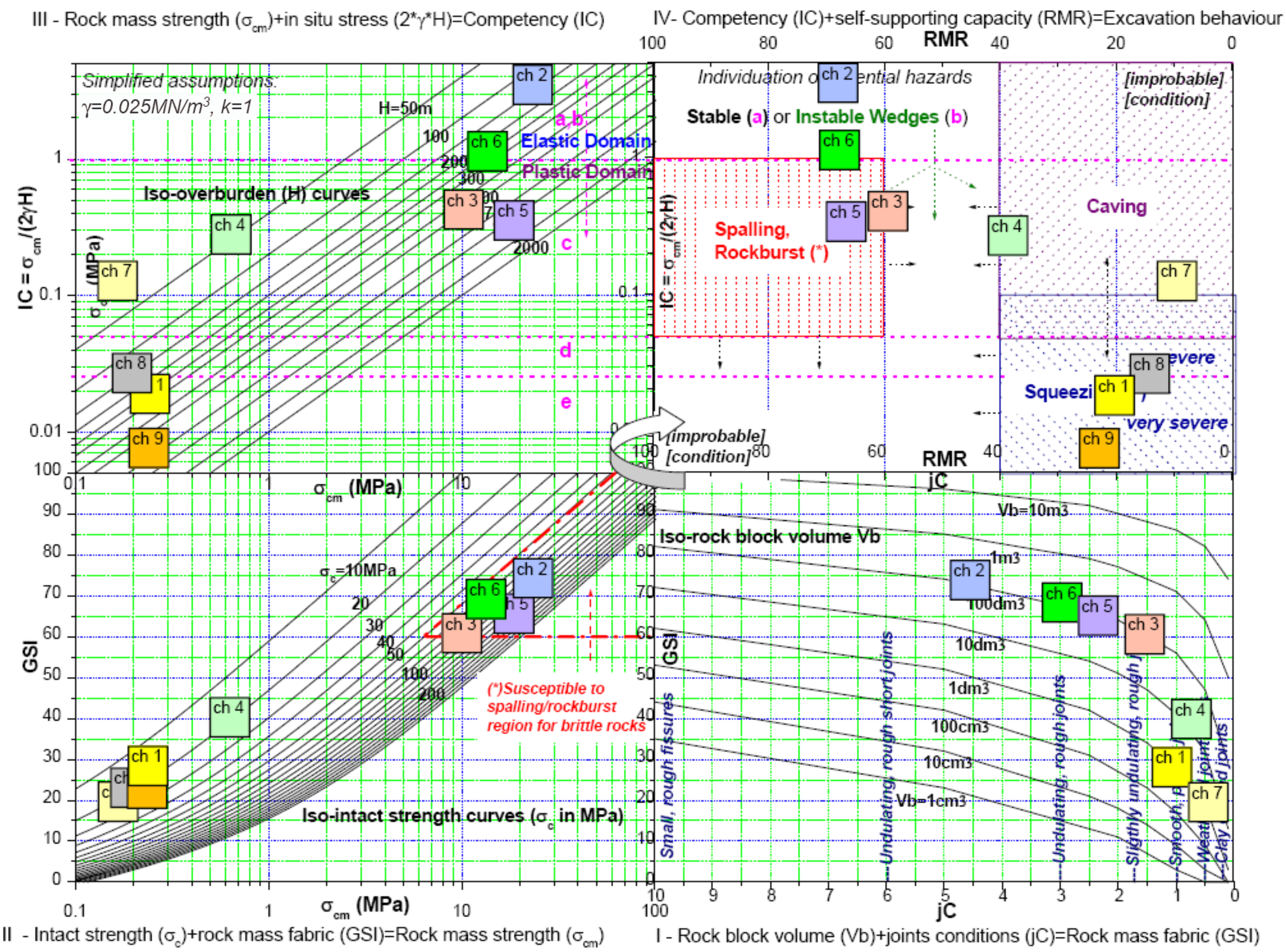

Fig.3.1: Example of practical application of the proposed multiple graph. The reference case histories (ch) are described in Tab.3.1. For ch3 and ch5, the assessment of GSI is just an approximate estimate on the basis of available information; for ch8 and ch9, the GSI is directly indicated in the II quadrant of the graph.

Fig. 3.2: Very severe squeezing behaviour in the S.Martin La Porte adit to the base tunnel of the new railway link Turin-Lyon (→case-history ch1): up to more than 2m of diametral convergence with consequent necessity of tunnel re-shaping (Photo: courtesy of J. Piraud (Antea)).

ch #	Source	Tunnel	Note (*hazard*)	Main Primary Stabilisation Measures
1	Geodata (2006)	S.Martin La Porte Adit (D~10m) to the Base tunnel of the new railway link Lyon-Turin [France] →Fig. 3.2	In the zone crossing carboniferous black schist, extremely severe *squeezing* condition during full face excavation (measured convergences up to 2m, which required re-shaping)	fbr (f/c); ovx; rb; ssrb+shd.
2	Geodata (2002)	Penchala [Malaysia] twin tube highway tunnel (D ~15m)	Ordinary advancement (full face) in good granite with negligible deformation (elastic-domain) and occasional *wedge* failures	dr; sp; rb+sh
3	GD-Test (2007)	Campegno [Italy] roadway tunnel (D ~12m)	Highly anisotropic stress conditions (k≈0.3), with principal stress inclined, parallel to the surface slope. Occasional *rockburst* in rhyolitic-porphyric rock mass during full-face excavation.	dh; sp(f); bl; be; srb+sh(fc)
4	Geodata (2007)	Montegrosso [Italy] roadway tunnel (D~13m)	Full-face excavation in poor schistose rock mass with some tendency to *caving*	dr; fbr(c); srb+sh
5	A.Anadón (2007)	Maule [Chile] hydroelectric system tunnel (D~8m) →Fig. 3.3	Heavy *rockburst* during full-face excavation in hard grain-diorite	sp; bl; rb+sh
6	Geodata (2005)	Menaggio [Italy] roadway tunnel (D=13.5m)	An exploratory tunnel by TBM was previously realized (D=4.2m) in the tunnel section. Advancement (full face) in good dolomitic limestone, with negligible deformation, but with intercepting of fractured/weathered layer	srb+sh
7	Geodata (2007)	Vispa [Italy] roadway tunnel (D~13m)	Full-face excavation in very poor weathered schist, with marked *caving* tendency	dr; fbr(f); ua; srb+sh
8	Geodata (2002)	Driskos [Greece] twin tube highway tunnel (D~12.5m)	Severe *squeezing* condition during bench excavation in silty-flysch with frequent band of highly tectonized rock mass, requiring additional stabilising measures and frequent re-shaping of the section	dr; srb+rb+sh; ca,..
9	Hoek and Marinos (2000)	Yacamboo [Venezuela] hydroelectric system tunnel (D~5m)	Extreme *squeezing* behaviour in very low strength graphitic phyllite at depths of up to 1200m	ovx; ssrb+shd;..

Tab.3.1: List of the reference Case-Histories (ch) and the relative stabilisation measures applied.
Note: be=anticipate bench excavation; bl=reduced blasting length and/or optimisation of the drilling scheme; ca=long cable anchor; dh=destressing blasting; dr=drainages in advancement; fbr (f/c) = pre-consolidation by cemented fibreglass (face/contour); ovx= over-excavation; rb = radial bolting; sh=shotcrete (fibre-reinforced or with steel mesh); shd= sh with deformable elements or gaps; sp=spiling in advancement with Swellex type bolts (f/c); srb=steel ribs; ssrb=sliding steel ribs; ua= umbrella arch with steel pipe.

Fig. 3.3: The dramatic sequence of heavy rock-burst occurred in the Maule Tunnel (Chile) during drilling. The tunnel was crossing hard grain–diorites with overburden of about 1000m (→case-history ch5). Note in the central photogram, the development of fracturing in the upper right part of the tunnel face. The elapsed time between the first and third photogram is less than 1sec (Video: courtesy of F.A. Anadon (Dragados))

4 CONCLUSION

A multiple graph for the preliminary estimate of the rock masses excavation behaviour and, consequently, of the probable hazards for tunnelling has been illustrated.

Such a prediction of the excavation response is obtained by means of the quantification, in a logical sequence, of (1) fabric, (2) strength, (3) competency and (4) self-supporting capacity of rock mass.

Despite the preliminary character of the prediction, which involves some simplified assumptions (for example, circular tunnel in homogeneous/isotropic rock mass, equivalent continuum modelling, k=1,..), the described method may be a useful tool, mainly in the first phases of design, for a quick identification of potential critical scenarios, as well as for performing sensitivity analysis, by means also of a probabilistic approach.

On the basis of such a preliminary analysis, the tunnel design can consequently focus on the detected potential problems, implementing with the required detail the most adequate methods of analysis and calculations.

5 BIBLIOGRAPHY

Abadía Anadón F. (2007): *Hard rock bursting phenomena in Maule tunnel (Chile)* Proc. I.S.R.M. Workshop "Underground Works under Special Conditions", Madrid

Bandis S.C. (1997): *Rock characterization for Tunnelling – A Rock Engineer's Perspective.* Feldsbau 15, Nr.3.

Bieniawski Z.T. (1984): *Rock Mechanics Design in Mining and Tunneling*. Balkema, Rotterdam, 272pp

Bieniawski Z.T. (1989): *Engineering Rock Mass Classification*, John Wiley & Son.

Cai M., Kaiser P.K., H., Tasaka Y. and Minami M. (2007): *Determination of residual strength parameters of jointed rock masses using the GSI system.* International Journal of Rock Mechanics & Mining Sciences 44 (2007) 247–265.

Carranza-Torres C. (2004): *Elasto-plastic solution of tunnel problems using the generalized form of the Hoek–Brown failure criterion*. Proceedings of the ISRM SINOROCK.

Diederichs M.S., Kaiser P.K. and Eberhards E. (2004): *Damage initiation and propagation in hard rock during tunnelling l and the influence of near-face stress rotation*. Int. Journal of Rock Mechanics and Mining Science n.41.

Diederichs M. (2005): *General Report: Summary of Meetings with Geodata with recommendations towards a Design Methodology for spalling Failure and Rockburst Hazards*. Personal communication to Geodata.

Hencher S.R. (1994): *Recognising the significance of complex geological conditions.* Tunnelling in difficult conditions. Politecnico di Torino: Quinto ciclo di conferenze di meccanica ed ingegneria delle rocce.

Hoek E. and Brown E.T. (1980). *Underground Excavations in Rock.* The Institution of Mining and Metallurgy, London, 527p.

Hoek E. and Diederichs M. (2006): *Estimation of rock mass modulus*. Int. Journal of Rock Mechanics and Mining Science.

Hoek E. and Marinos P., (2000): *Predicting Squeeze*. Tunnels and Tunnelling International, November, pp.45-51.

Marinos P. and Hoek E. (2001): *Estimating the geotechnical properties of heterogeneous rock masses such as Flysch* Bull. Engg. Geol. Env. 60, 85-92.

Hoek E., Carranza-Torres C. and Corkum B. (2002): *Hoek-Brown failure criterion – 2002 Edition*. Proc.North American Rock Mechanics Society. Toronto, July 2002.

Hoek E., Kaiser P.K. and Bawden W.F. (1995): *Support of Underground Excavations in Hard Rock.* Balkema, Rotterdam, 215pp.

Kaiser P.K. (1994): *Rockmass failure and implications for support design*. 5° Ciclo di Conferenze di Meccanica e Ingegneria delle Rocce a cura di G. Barla. Politecnico di Torino.

Kovari K. (1998): *Tunnelling in Squeezing Rock.* Tunnel n.5.

Palmstrom A. (1996): *Characterizing rock masses by the RMi for use in practical rock engineering*. Tunn. and Und. Space Tech. vol.11

Palmstrom A. (2000): *Recent developments in rock support estimates by the RMi*. Journal of Rock mechanics and tunneling technology, Vol.6, pp.1-9.

Russo G., Kalamaras G.S. and Grasso P. (1998): *A discussion on the concepts of geomechanical classes, behavior categories and technical classes for an underground projec*t. Gallerie e grandi opere sotterranee, N.54, pp.40-51.

Russo G. and Grasso P. (2006): *Un aggiornamento sul tema della classificazione geomeccanica e della previsione del comportamento allo scavo*. Gallerie e grandi opere sotterranee, N.80, pp.56-65.

Russo G. and Grasso P. (2007): *On the classification of the rock mass excavation behaviour in tunnelling* Proc. 11th Congress of ISRM, Lisbon, pp 979-982

Russo G. (2007): *Improving the reliability of GSI estimation: the integrated GSI-RMi system.* Proc. I.S.R.M. Workshop "Underground Works under Special Conditions", Madrid, pp 123-130

Russo G. (2008): *A new rational method for calculating the GSI.* Submitted to Tunnelling and Underground Space Technology.

Tzamos S. and Sofianos A.I. (2007): *A correlation of four rock mass classification systems through their fabric indices*. Intern. Journal of Rock Mechanics and Mining (in press)

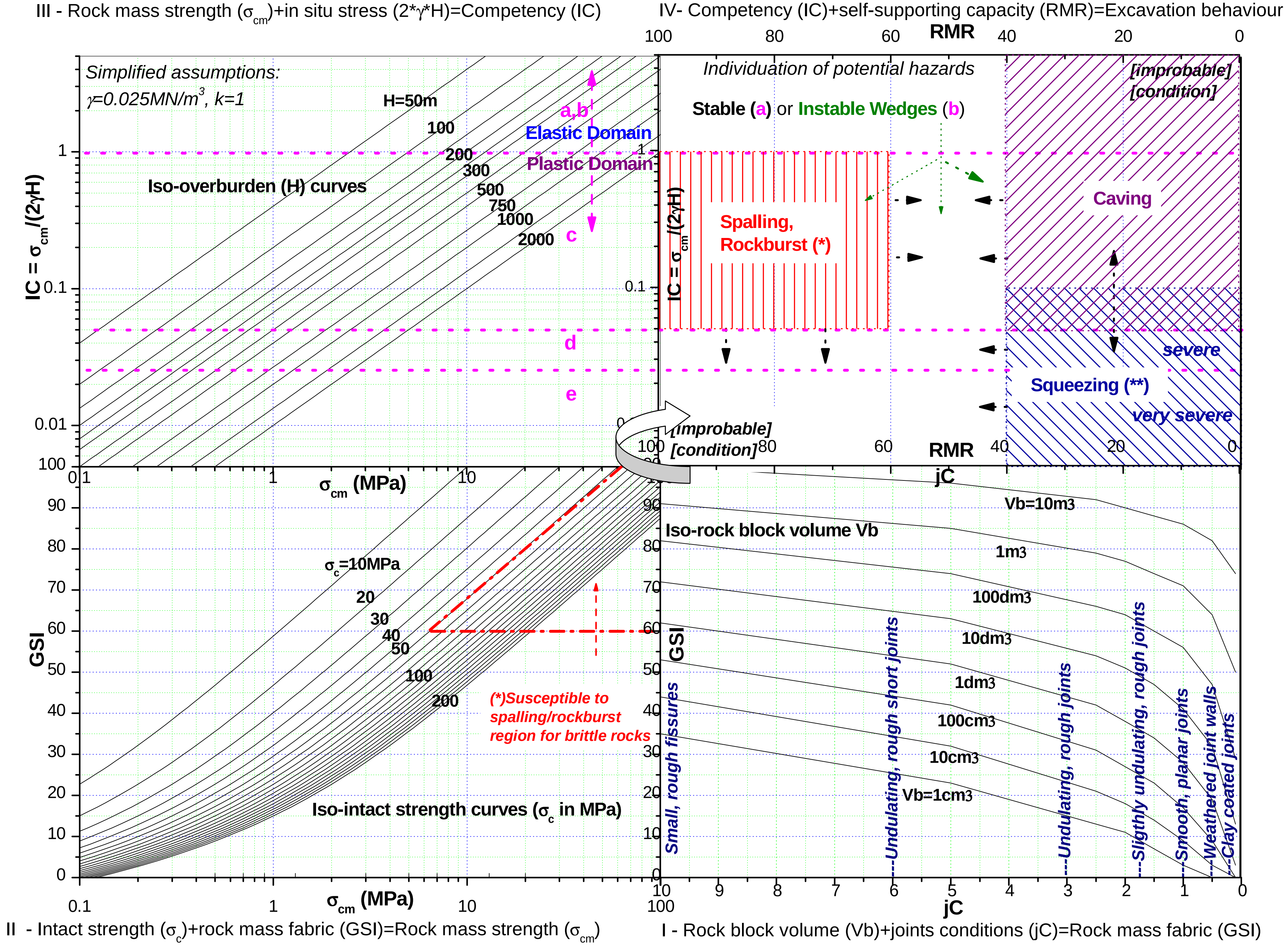

(*) only for the susceptible region, otherwise the development of plastic region and moderate radial convergences are more probable

(**) depending also from the length of the potential proned zone: given a possible "silo effect", for short zones included in good quality rocks, a caving behaviour it is most likely